

Toward a Pharmacophore for Drugs Inducing the Long QT Syndrome: Insights from a CoMFA Study of HERG K⁺ Channel Blockers

Andrea Cavalli,[†] Elisabetta Poluzzi,[‡] Fabrizio De Ponti,[‡] and Maurizio Recanatini^{*†}

Department of Pharmaceutical Sciences, University of Bologna, Via Belmeloro 6, I-40126 Bologna, Italy, and Department of Pharmacology, University of Bologna, Via Irnerio 48, I-40126 Bologna, Italy

Received March 25, 2002

In this paper, we present a pharmacophore for QT-prolonging drugs, along with a 3D QSAR (CoMFA) study for a series of very structurally variegated HERG K⁺ channel blockers. The blockade of HERG K⁺ channels is one of the most important molecular mechanisms through which QT-prolonging drugs increase cardiac action potential duration. Since QT prolongation is one of the most undesirable side effects of drugs, we first tried to identify the minimum set of molecular features responsible for this action and then we attempted to develop a quantitative model correlating the 3D stereoelectronic characteristics of the molecules with their HERG blocking potency. Having considered an initial set of 31 QT-prolonging drugs for which the HERG K⁺ channel blocking activity was measured on mammalian transfected cells, we started the construction of a theoretical screening tool able to predict whether a new molecule can interact with the HERG channel and eventually induce the long QT syndrome. This *in silico* tool might be useful in the design of new drug candidates devoid of the physicochemical features likely to cause the above-mentioned side effect.

Introduction

The long QT syndrome (LQTS) is characterized by the prolongation of the QT interval of the surface electrocardiogram and is associated with an increased risk of torsades de pointes, a ventricular tachyarrhythmia that may degenerate into ventricular fibrillation and sudden death.¹ Several congenital and acquired disorders can lead to prolongation of the QT interval; of special interest is the fact that numerous agents, belonging to different drug classes, have been associated with QT prolongation and occurrence of torsades de pointes. Recently, several regulatory interventions have involved drugs for which this potentially fatal risk was recognized only after marketing authorization.² Screening methods for the early detection of an effect on the QT interval are therefore required during the drug development process, and several *in vivo* and *in vitro* methods are now available.^{3,4}

The QT interval is defined as the time interval between the onset of the QRS complex and the end of the T wave and therefore includes both the ventricular depolarization and repolarization intervals. Although several pathophysiological mechanisms can lead to prolongation of the QT interval,^{5–7} the key mechanism for drug-induced QT prolongation is the increased repolarization duration through blockade of outward K⁺ currents (especially the delayed rectifier repolarizing current, *I_K*). In particular, most of the QT-prolonging drugs have been shown to inhibit the K⁺ channels encoded by the human ether-à-go-go related gene (HERG), at the basis of the rapid component of *I_{Kr}* named *I_{Kr}*.^{8–12} HERG K⁺ channel blockade is therefore the most

important mechanism through which QT-prolonging drugs increase cardiac action potential duration.¹³ Notably, blockade of HERG K⁺ channels forms the basis of the therapeutic effect of class III antiarrhythmic drugs, but for all other drugs, it is an unwanted side effect that must be detected as early as possible during drug development. IC₅₀ for inhibition of HERG K⁺ channels expressed in different cell lines is considered a primary test to study the QT-prolonging potential of a compound.¹⁴

Since none of the existing *in vitro* tests to assess the QT-prolonging potential of a compound has an absolute predictive value,⁴ the availability of *in silico* methods in the early phase of drug development would dramatically increase the screening rate and would also lower the costs compared to experimental assay methods. At the present time, to our knowledge, no theoretical screening method for the evaluation of QT-prolonging properties of molecules is publicly available. In an attempt to explore the possibility of building an *in silico* screening system based on the known structure–activity relationships (SAR) of LQTS-inducing noncardiac drugs, we report here a pharmacophore for such drugs, based on an initial set of molecules taken from an organized list of QT-prolonging compounds.¹⁵ Furthermore, we present a 3D QSAR model obtained by means of the CoMFA technique that attempts to correlate the physicochemical features of the drug molecules with their blocking activity toward the HERG K⁺ channel. The obtained CoMFA model was validated by predicting the biological activities of a set of molecules not used in deriving the 3D QSAR equations. We propose this model as a first step toward the development of a tool able to predict whether a molecule of pharmacological interest bears structural features likely to induce LQTS.

* To whom correspondence should be addressed. Phone: +39 051 2099720. Fax: +39 051 2099734. E-mail: mreca@alma.unibo.it.

[†] Department of Pharmaceutical Sciences.

[‡] Department of Pharmacology.

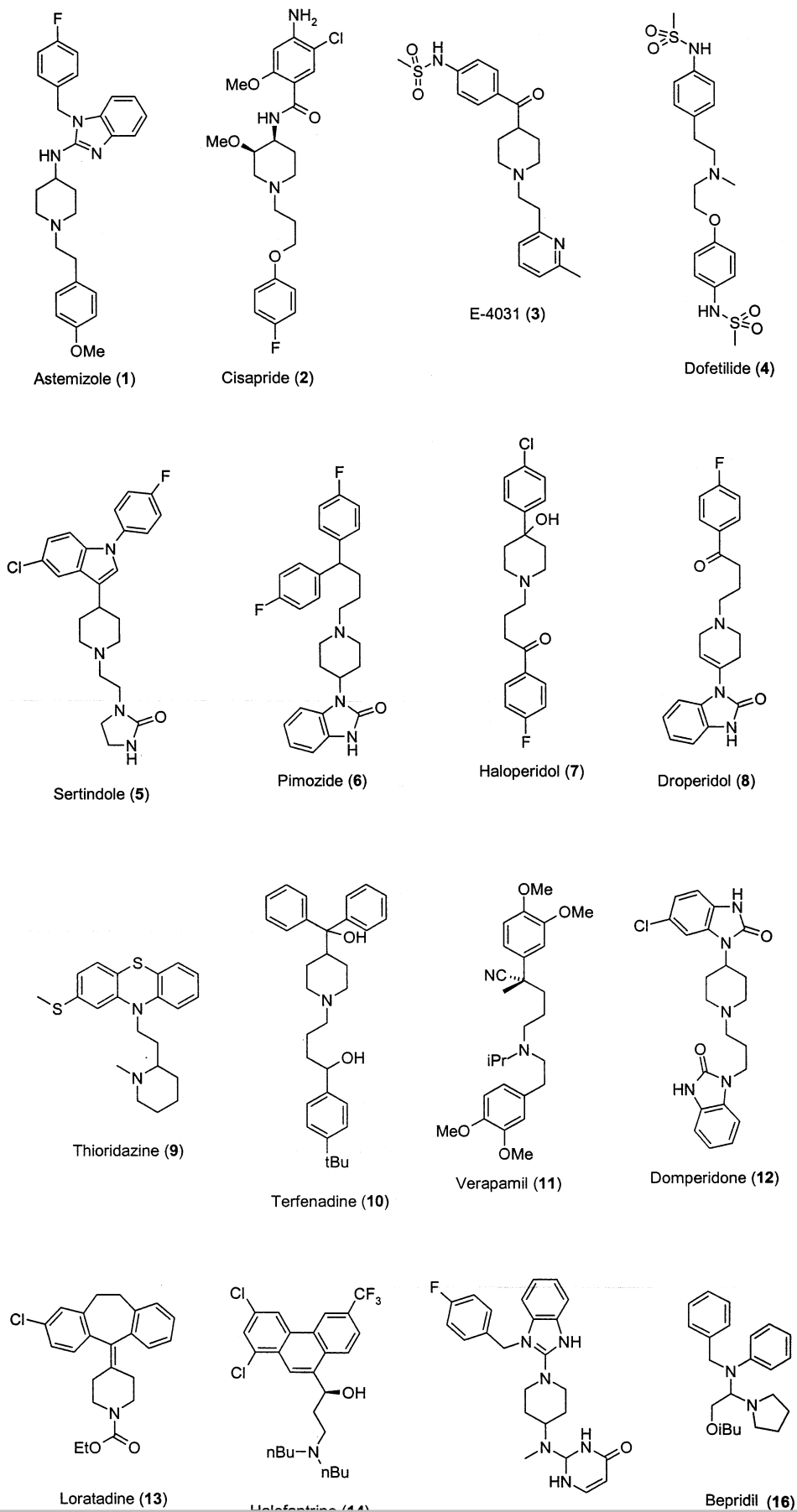
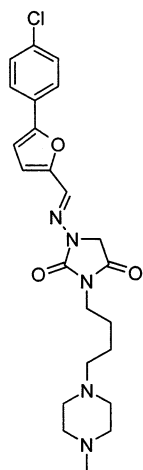
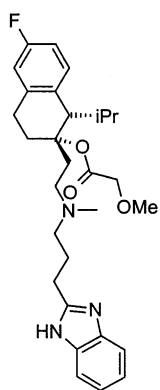
Chart 1. QT-Prolonging Drugs Considered in the Paper^a

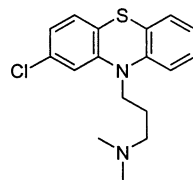
Chart 1 (Continued)



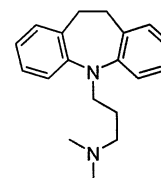
Azimilide (17)



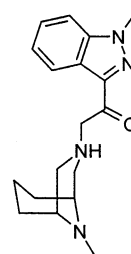
Mibefradil (18)



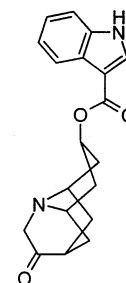
Chlorpromazine (19)



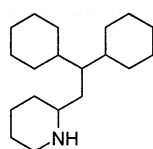
Imipramine (20)



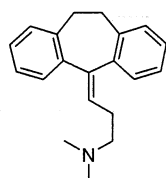
Granisetron (21)



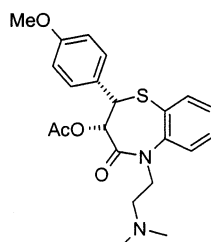
Dolasetron (22)



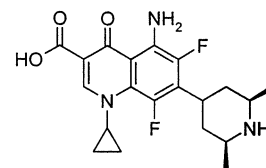
Perhexiline (23)



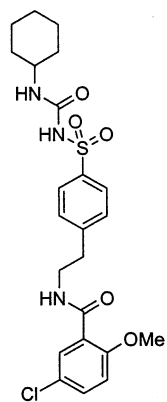
Amitriptyline (24)



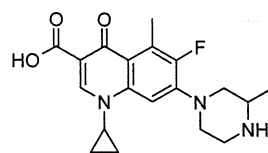
Diltiazem (25)



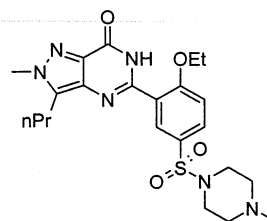
Sparfloxacin (26)



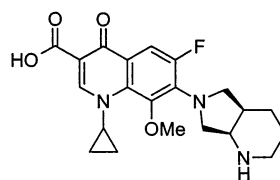
Glibenclamide (27)



Grepafloxacin (28)



Sildenafil (29)



Moxifloxacin (30)

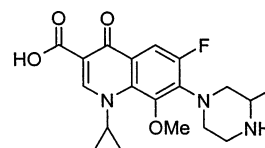
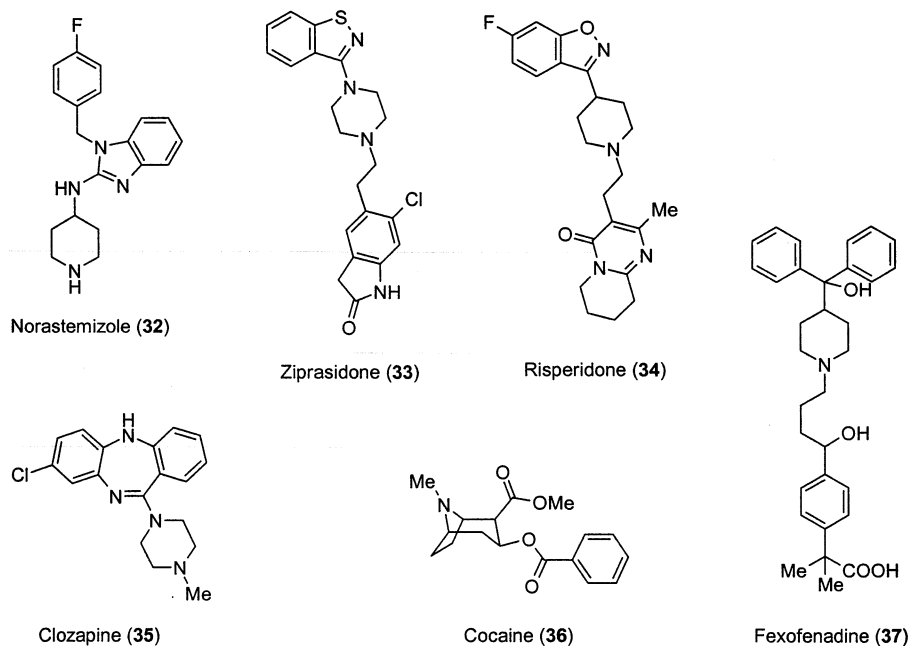


Chart 1 (Continued)



^a In the CoMFA analysis, compounds 1–31 and 32–37 were the training and the test sets, respectively.

Methods

1. QT Prolonging Drugs Selected for the Study.

In principle, a pharmacophore accounting for a certain pharmacological action should be built by taking into consideration all (or most) of the compounds able to elicit such an action. In the case of the QT-prolonging effect, besides the class III antiarrhythmic drugs, several other agents are known to induce this response and new entries are reported almost monthly at an accelerated pace. Indeed, prolongation of the QT interval by nonantiarrhythmic drugs is not an unusual finding, but the yet-unanswered question is to what degree QT prolongation has to be considered clinically significant. In this regard, in recent papers, we proposed a list of noncardiac QT-prolonging drugs, based on specific clinical and nonclinical criteria, and aimed to make a starting point to maintain a “consensus list” to be periodically updated.¹⁵ It seemed reasonable to consider this database (about 140 compounds at publication time) as the source of molecules to be used in the construction of the pharmacophore. However, since the pharmacophoric scheme must refer to a well-defined molecular target (i.e., the HERG K⁺ channel), we selected from the whole list only those drugs for which HERG K⁺ channel inhibition had been reported. The final set of molecules shown in Chart 1 was obtained by combining our list¹⁵ with Fenichel’s database,¹⁶ which also includes drugs used as antiarrhythmics; we selected only those drugs for which IC₅₀ values for inhibition of HERG K⁺ channels expressed in mammalian cells (HEK, CHO, COS, neuroblastoma cells; see Table 1) were available. We decided not to include IC₅₀ values obtained in nonmammalian cell lines, such as *Xenopus laevis* oocytes, since it is now recognized that the use of these systems leads to a significant underestimation of a drug’s potency as a HERG K⁺ channel blocker (the highly lipophilic environment in *Xenopus* oocytes limits

Table 1. Observed and Calculated HERG K⁺ Channel Blocking Activity of Compounds 1–31

compound	IC ₅₀ (nM)	pIC _{50obsd}	pIC _{50fit} ^a	Δ
astemizole (1)	0.9 ^b	9.04	8.53	0.51
cisapride (2)	6.5 ^b	8.19	7.96	0.23
E-4031 (3)	7.7 ^b	8.11	7.85	0.26
dofetilide (4)	9.5–15 ^b	7.91	7.67	0.24
sertindole (5)	14 ^b	7.85	8.04	−0.19
pimozide (6)	18 ^b	7.74	7.80	−0.06
haloperidol (7)	28.1 ^b	7.55	7.58	−0.03
droperidol (8)	32.2 ^b	7.49	7.82	−0.33
thioridazine (9)	35.7 ^b	7.45	7.23	0.22
terfenadine (10)	56–204 ^b	6.89	7.22	−0.33
verapamil (11)	143 ^b	6.84	7.05	−0.21
domperidone (12)	162 ^b	6.79	6.88	−0.09
loratadine (13)	173 ^b	6.76	5.83	0.93
halofantrine (14)	196.9 ^c	6.70	6.81	−0.11
mizolastine (15)	350 ^b	6.45	6.65	−0.20
bepridil (16)	550 ^d	6.26	6.30	−0.04
azimilide (17)	560 ^c	6.25	6.15	0.10
mibefradil (18)	1430 ^d	5.84	5.75	0.09
chlorpromazine (19)	1470 ^c	5.83	5.68	0.15
imipramine (20)	3400 ^c	5.47	5.98	−0.51
granisetron (21)	3730 ^b	5.42	5.64	−0.22
dolasetron (22)	5950 ^b	5.22	4.99	0.23
perhexiline (23)	7800 ^b	5.11	5.18	−0.08
amitriptyline (24)	10000 ^b	5.00	5.66	−0.66
diltiazem (25)	17300 ^b	4.76	5.02	−0.26
sparfloxacin (26)	18000–34400 ^c	4.58	4.39	0.19
glibenclamide (27)	74000 ^e	4.13	4.07	0.06
grepafloxacin (28)	50000–104000 ^c	4.11	4.35	−0.24
sildenafil (29)	100000 ^b	4.00	3.50	0.50
moxifloxacin (30)	103000–129000 ^c	3.93	3.82	0.11
gatifloxacin (31)	130000 ^c	3.89	4.16	−0.27

^a Calculated from the non-cross-validated CoMFA model. ^b In human embryonic kidney (HEK) cells. ^c In Chinese hamster ovary (CHO) cells. ^d In African green monkey kidney derived cell line COS-7. ^e In neuroblastoma cells.

Compounds 1–31 were used for the pharmacophore generation, and they also constituted the training set for the CoMFA procedure. In this connection, for each drug, the HERG blocking potency expressed as an IC₅₀ value is reported in Table 1. It is remarkable that the

To assess the predictive ability of the CoMFA model, we considered a test set of molecules (**32–37**, Chart 1) taken from Fenichel's list, or whose activity as a HERG K⁺ channel blocker was reported after the publication of our list (e.g., cocaine^{18,19}).

2. Molecular Modeling. Here, we describe the construction of the three-dimensional (3D) models of the molecules, the conformational search followed by a cluster analysis, the pharmacophore generation, and the 3D QSAR analysis based on the comparative molecular field analysis (CoMFA) procedure.²⁰ All the molecular modeling studies were carried out by means of the SYBYL²¹ and MacroModel²² software running on a Silicon Graphics workstation.

2.1. Construction of the Models. The 3D models of the molecules were either retrieved²³ from the Cambridge Structural Database (CSD),²⁴ or modeled by adding functional groups on crystallographic skeletons. Thus, very few models were built by assembling fragments retrieved from the standard SYBYL library. The following molecules were directly retrieved from the CSD (the CSD code is in parentheses): astemizole, **1** (ZENREP); cisapride, **2** (KEYOB); pimozone, **6** (PI-MOZD); haloperidol, **7** (HALOPB); droperidol, **8** (KAMCIK); thioridazine, **9** (WAVCEB); verapamil, **11** (CURHON); domperidone, **12** (BEQJUC); loratadine, **13** (YOVZEO); halofantrine, **14** (SATRAG); bepridil, **16** (CEZBAK); chlopromazine, **19** (DUKTOS); imipramine, **20** (IMIPRB); perhexiline, **23** (DEPGUA01); amitriptyline, **24** (YOVZEO); diltiazem, **25** (CEYHUJ01); sparfloxacin, **26** (COQWOU); glibenclamide, **27** (DUNXAL); sildenafil, **29** (CAXZEG); risperidone, **34** (WASTEP); clozapine, **35** (CMPDAZ10); and cocaine, **36** (COCAIN10). The following molecules were built by adding fragments to crystallographic skeletons: E-4031, **3**, was built starting from BERGUA; terfenadine, **10**, from YIHJOO; mizolastine, **15**, from CELNUG and LEJKUG; azimilide, **17**, from LIAXBUD; mibefradil, **18**, from BZDMAZ; granisetron, **21**, from KUSZED; dolasetron, **22**, from KAMCIK; grepafloxacin, **28**, and moxifloxacin, **30**, from NIVQAK; gatifloxacin, **31**, from COQWOU; ziprasidone, **33**, from DEDCIY, NUXWAE, and JIVAO. Norastemizole (**32**) and fexofenadine (**37**) are metabolites of astemizole (**1**) and terfenadine (**10**), respectively, and were built by modifying the structure of the parent compounds. Finally, only two molecules were built de novo, namely, dofetilide, **4**, and sertindole, **5**.

The molecular models obtained were first energy-minimized by using steepest descent and conjugate gradient until a convergence of 0.005 kJ mol⁻¹ Å⁻¹ on the gradient was reached. Then, conformational searches were carried out in order to sample the potential energy surface. All of the classical molecular mechanics calculations were performed by using the MMFF force field,^{25,26} which carries parameters for all the investigated molecules. Finally, the average conformers obtained from a cluster analysis (see below) were optimized by using the semiempirical Hamiltonian PM3²⁷ as implemented in the SYBYL package (keywords GNORM = 0.001, MMOK when needed).

2.2. Conformational Search. The conformational space of each molecule was sampled by means of Monte

behavior of a molecule is simulated by randomly changing dihedral angle rotations or atom positions. Then, the trial conformation is accepted if its energy has decreased from the previous one. If the energy is higher, various criteria can be applied to determine whether the new conformation should be accepted or not. In our simulations, all of the dihedral angles of single linear bonds were allowed to move freely, and the trial conformation was accepted if the energy was lower than that of the previous conformation or if the energy was within a fixed energy window (100 kJ/mol). The number of Monte Carlo trials was set equal to 7000. A high number, usually in the order of hundreds, of conformers was generated. To classify the conformations obtained for each molecule, a geometrical cluster analysis was carried out on the output of Monte Carlo searches.

2.3. Cluster Analysis. Generally, a cluster analysis²⁹ provides for the most significant solutions, by using filtering screens based on one or more external criteria. Conformations were classified in terms of geometrical similarity, and in particular, two conformers were considered as belonging to the same family when the heavy atom's root-mean-square displacement (rmsd) was lower than 1 Å. In this way, between 10 and 20 families of conformers were generated for each molecule, and the average structure of each family was energy-minimized and used in the procedure of pharmacophore generation.

2.4. Pharmacophore Generation. An inspection of molecules **1–31** of Chart 1 shows that they are widely varied from a structural point of view, which implies an objective difficulty in the search for a common pharmacophore. To tackle this problem, we adopted a "constructionist" approach to the pharmacophore generation, consisting of the individuation of an initial reference structure (the template) onto which we overlapped molecules starting from those with similar geometric and spatial characteristics. This superimposition procedure led to the individuation of further pharmacophoric characteristics that were then used to add the most different molecules and to refine the initial alignment. The template chosen for this study was the crystal structure of astemizole (**1**), because this molecule is one of the most potent long QT-inducing drugs, and HERG channel blockers (IC₅₀ = 0.9 nM, Table 1). The astemizole crystal structure was directly retrieved from the CSD and then geometrically optimized by means of PM3. Initially, three pharmacophoric points on the astemizole molecule were defined, namely, the basic nitrogen of the piperidine cycle (N) and the centers of mass (centroids C0 and C1) of the two close aromatic moieties. However, considering that several molecules of the training set bear an aromatic group connected to the basic nitrogen, a fourth pharmacophoric point was defined as the centroid (C2) of the phenyl ring belonging to the *N*-(*p*-methoxyphenylethyl) substituent of astemizole. Onto this template, the best-fitting conformer (within 20 kJ/mol from the global minimum) of the other molecules was then superimposed by using the corresponding pharmacophoric functions.

Not all the molecules displayed all four pharmacophoric points, and in such cases, the superimposition was

Explore Litigation Insights

Docket Alarm provides insights to develop a more informed litigation strategy and the peace of mind of knowing you're on top of things.

Real-Time Litigation Alerts



Keep your litigation team up-to-date with **real-time alerts** and advanced team management tools built for the enterprise, all while greatly reducing PACER spend.

Our comprehensive service means we can handle Federal, State, and Administrative courts across the country.

Advanced Docket Research



With over 230 million records, Docket Alarm's cloud-native docket research platform finds what other services can't. Coverage includes Federal, State, plus PTAB, TTAB, ITC and NLRB decisions, all in one place.

Identify arguments that have been successful in the past with full text, pinpoint searching. Link to case law cited within any court document via Fastcase.

Analytics At Your Fingertips



Learn what happened the last time a particular judge, opposing counsel or company faced cases similar to yours.

Advanced out-of-the-box PTAB and TTAB analytics are always at your fingertips.

API

Docket Alarm offers a powerful API (application programming interface) to developers that want to integrate case filings into their apps.

LAW FIRMS

Build custom dashboards for your attorneys and clients with live data direct from the court.

Automate many repetitive legal tasks like conflict checks, document management, and marketing.

FINANCIAL INSTITUTIONS

Litigation and bankruptcy checks for companies and debtors.

E-DISCOVERY AND LEGAL VENDORS

Sync your system to PACER to automate legal marketing.